Use of Giovanni with Ocean Color Time-Series Project Data for Trend Detection in the Coastal Zone

Acker, James[1]; Gregg, Watson[2]; Leptoukh, Gregory[1]; Kempler, Steven [1]; Casey, Nancy[2], Feldman, Gene[3]; McClain, Charles[3]; Esaias, Wayne[2]; Shen, Suhung[1]

[1]NASA Goddard Earth Sciences DISC NASA GSFC Code 610.2, Greenbelt, Maryland, 20771, USA;
[2]NASA GSFC Code 610.1, Greenbelt, Maryland, 20771, USA;
[3]NASA GSFC Code 614.8, Greenbelt, Maryland, 20771, USA

Abstract: Analysis of Sea-viewing Wide Field-of-view Sensor (SeaWiFS) chlorophyll concentration data from 1998 to 2003 indicated an increasing trend of 4% globally, with the increase occurring primarily in the coastal zone (Gregg et al. 2005). As numerous studies exist which have linked increased fluxes of nutrients to coastal waters from rivers and estuaries to higher chlorophyll concentrations and coastal eutrophication, it is expected that coastal chlorophyll concentrations will exhibit increasing trends with variability linked to precipitation and freshwater flux to the coastal zone. Acker et al. (2005) employed the GES DISC Interactive Online Visualization ANd aNalysis Infrastructure (Giovanni) to observe a strong chlorophyll response to markedly different flow conditions at the mouth of Chesapeake Bay in 2002 and 2003. More recent observations have determined a large chlorophyll concentration anomaly in November 2005 on the northeast coast of the United States apparently linked with near-record autumnal precipitation. In this study, Giovanni will be used to regionally characterize chlorophyll concentration trends in the coastal zone utilizing Ocean Color Time-Series Project data, and to examine differences between areas which are influenced by freshwater flow and areas with minimal influence of freshwater flow.

INTRODUCTION

The availability of oceanographic remote sensing data sets of increasing temporal length and significantly improved observational continuity invites synoptic investigations of trends which may exist within such data sets. Such investigations implicitly rely on improved data quality and accuracy. The Ocean Color Time-Series Project is creating a single data set spanning multiple missions and several decades, which allows for the investigation of trends in chlorophyll concentration and related optical parameters. The full Ocean Color Time-Series Project data set will begin with the Coastal Zone Color Scanner (CZCS) mission in 1978 and extend to the current Sea-viewing Wide Field-of-view Sensor (SeaWiFS) and Moderate Resolution Imaging Spectroradiometer (MODIS) mission onboard the Aqua platform (MODIS-Aqua). Construction of this data set will allow for further extension with subsequent ocean color remote sensing missions.

While awaiting the completion of the multi-mission, multi-decade Ocean Color Time-Series, the current nine-year long ocean color data set from the SeaWiFS mission provides the best opportunity to discover and investigate trends. Determination of trends within the SeaWiFS data set is facilitated by “Giovanni”, the Goddard Earth Sciences Data and Information Services Center (GES DISC)

Interactive Online Visualization ANd aNalysis Infrastructure. Giovanni provides rapid online analytical and visualization capability for SeaWiFS and MODIS-Aqua ocean color Level 3 (global) data products.

The marine coastal zone is a vitally important sector of the global oceanic environment for several reasons. A large percentage of global ocean primary productivity takes place in the coastal zone, due to increased nutrient availability either from terrestrial input (rivers) or from coastal upwelling systems. Estuarine areas provide nursery areas for larval fish and benthic fauna, and are important economically for seafood production, shipping and transportation, and recreation. Many coastal and estuarine areas are increasingly exploited as desirable areas for human habitation, leading to increasing population pressures. Furthermore, it is well-known that the coastal zone can be vulnerable to sever impacts from natural disasters such as coastal storms, hurricanes, and tsunamis, and from man-made disasters like oil spills and other forms of noxious pollution. Heavy nutrient inputs from agriculture in major river systems, and also vehicular exhaust from metropolitan areas, have been implicated in the observation of larger areas of coastal eutrophication and benthic hypoxia and anoxia. Such impacts degrade the desirability of the coastal zone, threaten its ecological integrity, and reduce its economic viability.

For the reasons described above, the determination of ocean color data trends in the coastal zone is likely to be of significant value to a variety of interests that are connected to the coastal zone. This study will demonstrate the simplicity of generating and evaluation chlorophyll *a* (chl *a*) concentration trends in several different coastal settings using SeaWiFS data and Giovanni. It is expected that such a demonstration can facilitate the utilization of this data in comprehensive studies of the coastal zone, allowing elucidation of the factors and processes that contribute to the perceived and anticipated trends. The integration of remote sensing observations with *in situ* data (ship, observational networks, data buoy, etc.) will improve our understanding of the processes affecting the health and integrity of the marine coastal zone.

STUDY METHODOLOGY

To examine trends in the coastal zone, several small regions were selected where the influence of major river systems was either expected to be significant, i.e. the regions were near major river outflow zones, or regions which were not adjacent to a significant river system. A few regions were selected to check on the integrity of the analysis by comparison to the results of Gregg et al. 2005. Figure 1 shows the selected regions superimposed on Figure 1 from Gregg et al. 2005, which displays areas with positive and negative chl *a* trends for the period 1998-2003.

Giovanni was used to create the regional boundaries and to define the temporal period of analysis. For each region, a time series of SeaWiFS monthly data was created for the period January 1998 to December 2005. Several area plots were created simultaneously to show the range of chl *a* in the region averaged over the full time period. After the time series was created, the average monthly values for the designated region were obtained using the ASCII data output function, imported to an Excel spreadsheet, and a time series with linear line fit was generated. The linear least-squares fit equation describing the line was generated simultaneously. The average monthly values were also used to calculate the statistical significance (P-value) for each time series (Zar 1976).

Giovanni utilizes the Grid Analysis and Display System (GrADS) to perform its averaging functions. To generate area average values for a data product over a specified region, the GrADS function *aave* is utilized. *aave* provides an area-weighted average for the entire specified region. *aave* performs latitudinal weighting by the difference between the sines of the latitude at the northern and southern edges of the grid box, and longitudinal weighting by the interval between the two adjacent grid points. Missing data values are not used to calculate the average.

RESULTS

Figures 2-8 show the specified regions selected for time series generation, and the resulting time series with the least-squares linear line fit. The slope of the least-squares fit line for each time-series is included in the figure. The results for each region are summarized below, in terms of the slope of the fitted line and the P-value of each time series. For purposes of comparison, most of the time series were plotted with a Y-axis scale between 0 and 3 milligrams per cubic meter (mg m^{-3}). The regions requiring a Y-axis with higher chl *a* values were the Amazon River Outflow, the northern Adriatic Sea, and the Congo River outflow. "Neutral" slopes are between +0.0005 and -0.0005. "Small positive" slopes are between +0.0006 and +0.0015, and "positive" slopes are larger than +0.0015. "Small negative" slopes lie between -0.0006 and -0.0015, and "negative" slopes have larger negative slopes than -0.0015. P values are shown in bold following the slope value; a P-value < 0.05 indicates a statistically significant trend at the 95% confidence level.

- Region 1, Pearl River Outflow — Small positive slope, — +0.0007 — **0.474**
- Region 2, Central China coast — Neutral slope — -0.0001 — **0.941**
- Region 3, Coastal Japan — Small positive slope, — +0.0012 — **0.322**
- Region 4, Straits of Tasmania — Small negative slope — +0.0006 — **0.110**
- Region 5, Southern Washington — Neutral slope — -0.0003 — **0.841**
- Region 6, Northern Oregon — Positive slope — +0.0015 — **0.274**
- Region 7, Central Oregon — Positive slope — +0.0033 — **0.082**
- Region 8, South Texas coast — Positive slope — +0.0015 — **0.014**
- Region 9, Mississippi River Outflow — Negative slope — -0.0034 — **0.056**
- Region 10, Chesapeake Bay South — Small positive slope — +0.0014 — **0.264**
- Region 11, Onslow Bay — Neutral slope — -0.0001 — **0.871**
- Region 11 (first 6 months excluded) — Positive slope — +0.0017 — **0.025**
- Region 12, Northern Chile — Positive slope — +0.0053 — **0.00002**
- Region 13, Amazon River Outflow — Negative slope — -0.0047 — **0.235**
- Region 14, Brazil South coast — Neutral slope — +0.0002 — **0.110**
- Region 15, Benguela Upwelling Zone — Negative slope — -0.0048 — **0.023**
- Region 16, Congo River Outflow — Positive slope — +0.0085 — **0.454**
- Region 16 (final 6 months excluded) — Negative slope — -0.0046 — **0.612**
- Region 17, South of France — Small negative slope — -0.0006 — **0.541**
- Region 18, Portugal North — Small negative slope — -0.0006 — **0.440**
- Region 18, Portugal South — Small negative slope — -0.0007 — **0.411**
- Region 19, North Sea — Negative slope — -0.0021 — **0.084**
- Region 20, Northern Adriatic Sea — Negative slope — -0.0114 — **0.011**

Region 12, Northern Chile, and Region 19, North Sea, were specifically chosen for comparison to the reported trends in Gregg et al. 2005. For all other cases, the specified regions were selected without reference to the results of Gregg et al. 2005. This process therefore resulted – accidentally – in a distribution of selected regions with no apparent statistically significant trends in chl *a* as reported by Gregg et al. 2005, with the exception of the two African coastal regions in the Congo River Outflow and the Benguela Upwelling Zone. In many of these regions, however, patterns seen in the time series over the time period of record and associated low P-values in the range 0.051 – 0.15 indicate potential trends that are candidates for further investigation. Further investigation could identify processes contributing to a potential trend in chl *a* concentrations.

DISCUSSION

The following discussion will briefly discuss the time series appearing in each figure.

The Western Pacific (Figure 2) has three selected regions: Pearl River Outflow, Central China coast, and Coastal Japan. The Pearl River outflow has a small positive slope, possibly indicating a riverine influence. The Central China coast region has a neutral slope. Perhaps the most surprising pattern is for the Coastal Japan region, which displays a clear seasonal pattern and where the small positive slope appears to be caused primarily by increasing seasonal peak monthly chl *a* concentrations. None of these regions had a low P-value.

There is only one selected region in the Straits of Tasmania (Figure 3). While moderately variable, there is only a small negative slope over the time period. The P-value for this time series was 0.110, a low value indicating a potential trend.

The Pacific Northwest (Figure 4) has three selected regions, chosen for close contiguity. These regions were chosen to investigate the possible influence of the Columbia River. No influence is apparent: the region farthest from the river, Central Oregon, has the largest positive slope and the lowest P-value. The regions closer to the river, Northern Oregon and Southern Washington, have lesser slopes. Seasonality is evident in the Central and Northern Oregon time series and is not as noticeable in the Southern Washington time series.

The Eastern United States (Figure 5) has four selected regions. South Texas has a positive slope and no apparent seasonal pattern. The P-value of 0.014 indicates a statistically significant positive trend. The Mississippi River Outflow region does display a seasonal pattern, and also has a clearly negative slope, with a P-value of 0.056, just below the 95% confidence level. This negative trend is somewhat unexpected, given the presence of a seasonal benthic zone of hypoxia and anoxia in the region due to high levels of primary productivity. Further observation of this region is warranted to determine if nutrient levels are also decreasing, or if there are other causes of the negative slope.

The Chesapeake Bay South region was chosen due to the observations of Acker et al. 2005, who reported a clear coupling of freshwater flow into the Bay with increased chlorophyll concentrations at the mouth of the Bay, likely due to increased availability of nitrate. There is only a small positive slope, so despite the influence of flow from the Bay on the adjacent oceanic waters, there is no evidence of an increasing influence.

The Onslow Bay region (Region 11) demonstrates the importance of anomalous events for the detection of trends in a time series. In February 1998, the Onslow Bay region had a very high monthly chl *a* concentration. For the full time series which includes this month, the region has a neutral slope. However, if the first six months of 1998 are excluded from the analysis, there is a distinct positive slope and the P-value markedly decreases to a statistically significant value of 0.025. This intriguing observation indicates that anomalous events can significantly affect trend detection in a time series analysis, and also indicates the advisability of investigating causation of anomalous events which are observed in a time series.

For South America (Figure 6), the first region, Northern Chile, was chosen with regard to the results of Gregg et al. 2005. This region, as indicated by Gregg et al.'s results, does have a clear positive slope and a very low P-value indicating high statistical significance. This region is south of the Peru Upwelling Zone, and there does not appear to be a signal from El Niño or La Niña events. The second region, the Amazon River Outflow, has a negative slope. Areas to the north and east of this region are indicated to have a positive trend by Gregg et al. 2005, but this region was closer to the coast. The difference in the slope here and the trends in the adjacent open ocean indicate the complexity of mixing processes affecting the Amazon River outflow plume.

The oligotrophic waters of the Brazil South region have very low chl *a* concentrations. The slope of the time series is neutral and the P-value of 0.110 indicates a potential trend. There is an interesting seasonal pattern in these data, similar to the pattern for Coastal Japan. From 2001 to 2005, the peak monthly seasonal chl *a* concentration increased steadily. Further investigation is required to determine if this pattern is persistent. The data record available for this study ended in June 2006, and the peak monthly concentrations occurred in either June or July. Gregg et al. 2005 reported negative chl *a* concentration trends in the adjacent South Atlantic Gyre, so the pattern observed for the Brazil South region may reflect a terrestrial influence.

The West African Coast (Figure 7) has two selected regions, in the Benguela Upwelling Zone and Congo River outflow. Gregg et al. 2005 reported decreasing chl *a* concentration trends in the Benguela Upwelling Zone, and this trend is also seen here as a negative slope for the selected region ($P = 0.023$). The Congo River outflow region also demonstrates the importance of anomalous events for time series trend analysis. In July 2005, a remarkably high chl *a* concentration in excess of 25 mg m^{-3} is observed for this region. If this month is included in the full time series, the region has a strong positive slope. However, if this event is excluded by removing the final six months of the time series, the region has a negative slope. Neither time series has a statistically significant P-value. (Further investigation is required to determine if the data value for July 2005 is valid.) Gregg et al. 2005 displays small areas of positive chl *a* trends in this region, but this is a region similar to the outflow of the Amazon River where the mixing of a large freshwater flow volume with marine waters creates a complex interaction.

Five regions were selected for Europe (Figure 8). The South of France region is east of the Rhone River delta, and has only a small negative slope, and the time series has a distinct seasonal pattern. Two adjacent regions were examined on the coast of Portugal, but no significant slopes were observed for either region. The North Sea region was chosen with regard to Gregg et al. 2005, and the expected negative slope is observed in the time series, with a low P-value of 0.084. This value indicates lower significance than would be expected for regions where Gregg et al. 2005 reported significant trends. This may be due to the region location, slightly east of areas where Gregg et al. reported significant negative trends.

The final region, the Northern Adriatic Sea, displays a definite negative slope and a P-value of 0.011. This region should be strongly influenced by the flow of the Po River, and is worthy of further investigation to determine if freshwater flow into the northern Adriatic has declined over the time period. Noxious phytoplankton blooms have also been reported in this region, and it is possible that species shifts influence the magnitude of chl *a* concentration here.

In summary, this study demonstrates the capability of Giovanni to rapidly provide time series of chl *a* for many different and diverse regions, establishing baselines for further investigations with related oceanographic data sets. Several intriguing patterns are observed in the time series shown in this study, particularly declining trends in high productivity areas – both river outflow and upwelling zones – and increasing seasonal peak concentrations on the coasts of Japan and Brazil. The time series data that can be generated rapidly with Giovanni (including improved time resolution with 8-day data sets) provide vital information for monitoring regional coastal changes and trends.

REFERENCES

Acker, J., Harding, L., Leptoukh, G., Zhu, T. and Shen, S. "Remotely-sensed chl a at the Chesapeake Bay mouth is correlated with annual freshwater flow to Chesapeake Bay", GEOPHYSICAL RESEARCH LETTERS, VOL. 32, L056001, doi: 10.1029/2004GL021852, 2005.

Gregg, W., Casey, N., and McClain, C. "Recent Trends in Global Ocean Chlorophyll", GEOPHYSICAL RESEARCH LETTERS, VOL. 32, L03606, doi:10.1029/2004GL021808, 2005.

Zar, J.H., *Biostatistical Analysis*, 3rd Ed., Prentice-Hall, Upper Saddle River, NJ, 1976.

Figure 1

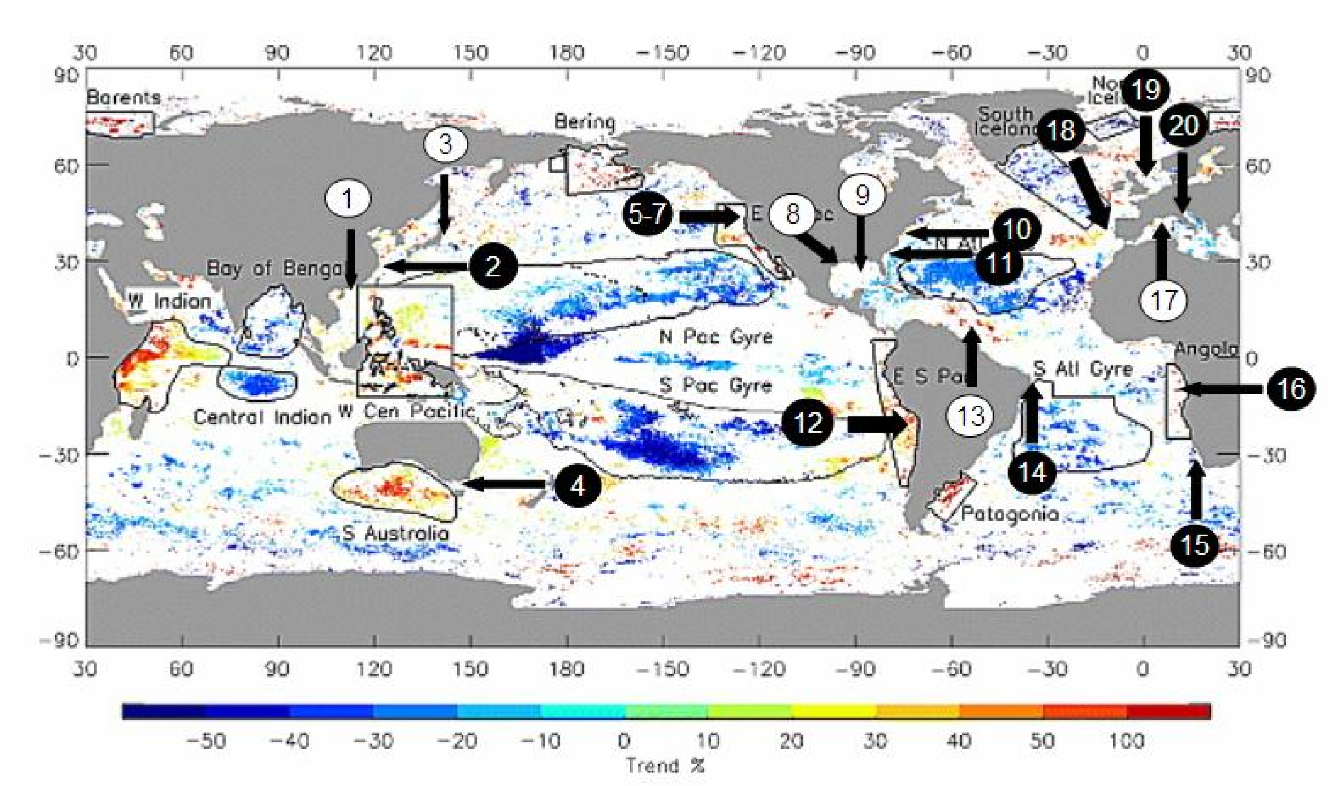

Barents
Bering
Bay of Bengal
W Indian
Central Indian
W Cen Pacific
N Pac Gyre
S Pac Gyre
S Australia
E S Pac
S Atl Gyre
Angola
Patagonia
South Iceland
N Atl
Trend %

Figure 2

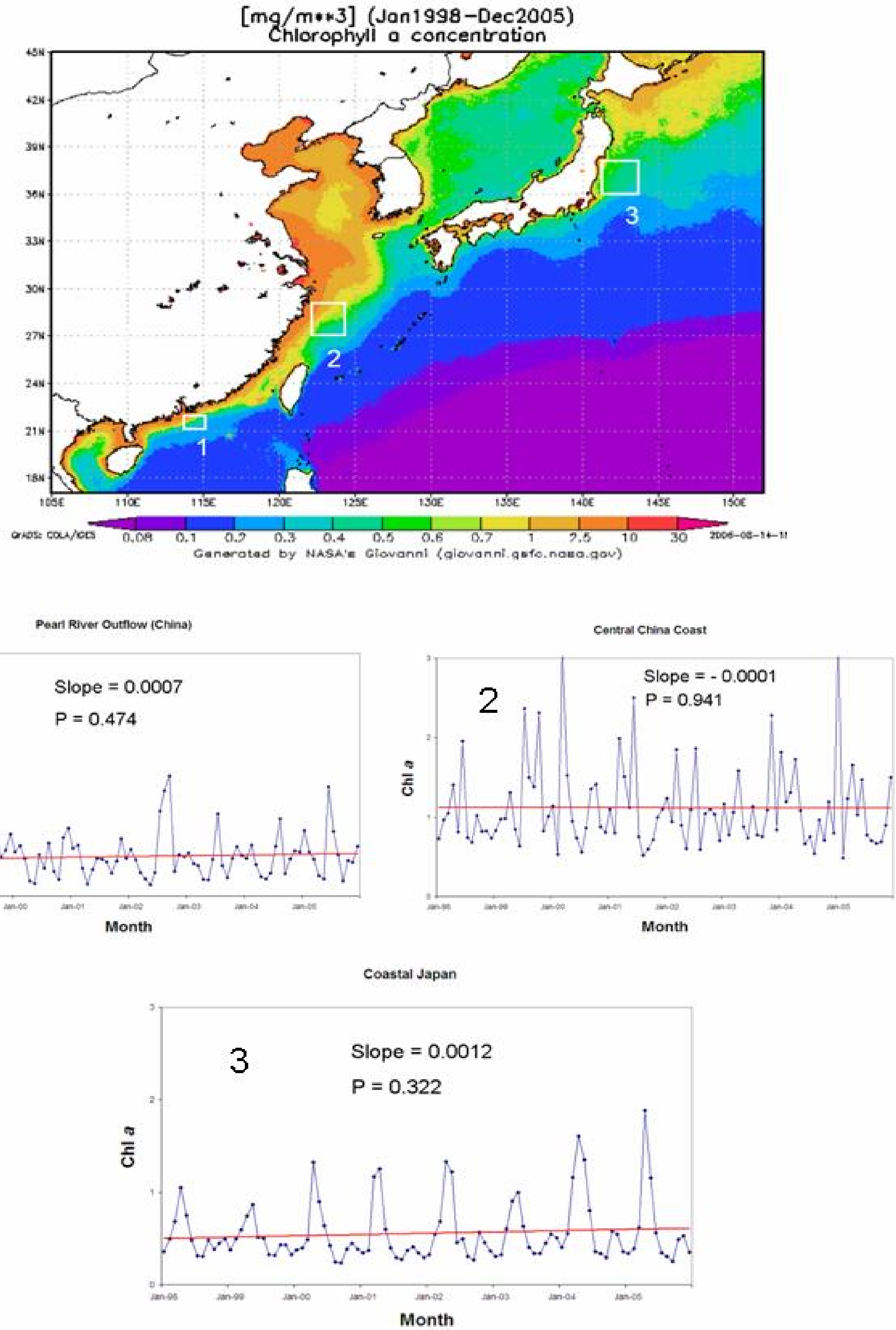

[mg/m**3] (Jan1998–Dec2005)
Chlorophyll a concentration
1
2
3
Generated by NASA's Giovanni (giovanni.gsfc.nasa.gov)
Pearl River Outflow (China)
Slope = 0.0007
P = 0.474
Chl a
Month
Central China Coast
Slope = - 0.0001
P = 0.941
Chl a
Month
Coastal Japan
Slope = 0.0012
P = 0.322
Chl a
Month

Figure 3

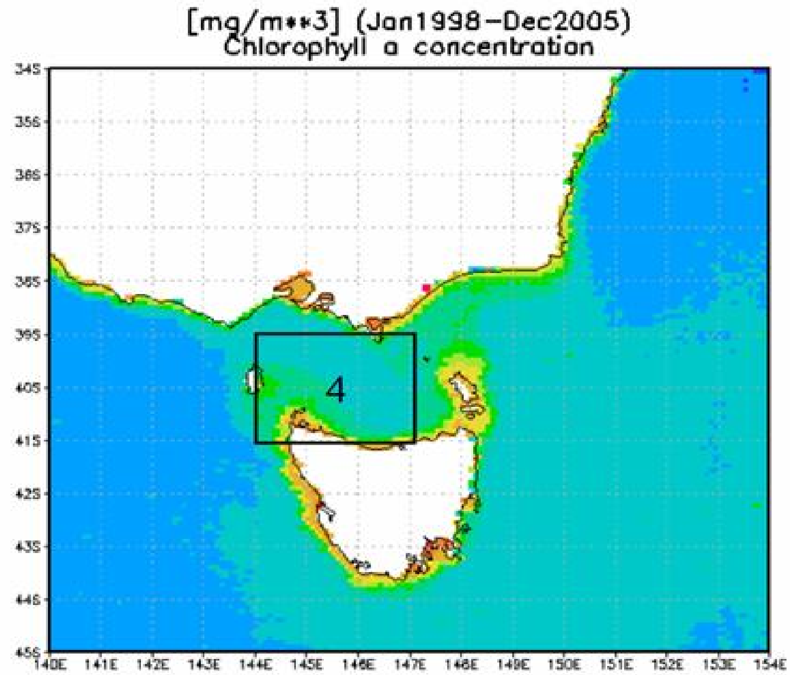
[mg/m**3] (Jan1998–Dec2005)
Chlorophyll a concentration
34S
35S
36S
37S
38S
39S
40S
41S
42S
43S
44S
45S
140E
141E
142E
143E
144E
145E
146E
147E
148E
149E
150E
151E
152E
153E
154E
4

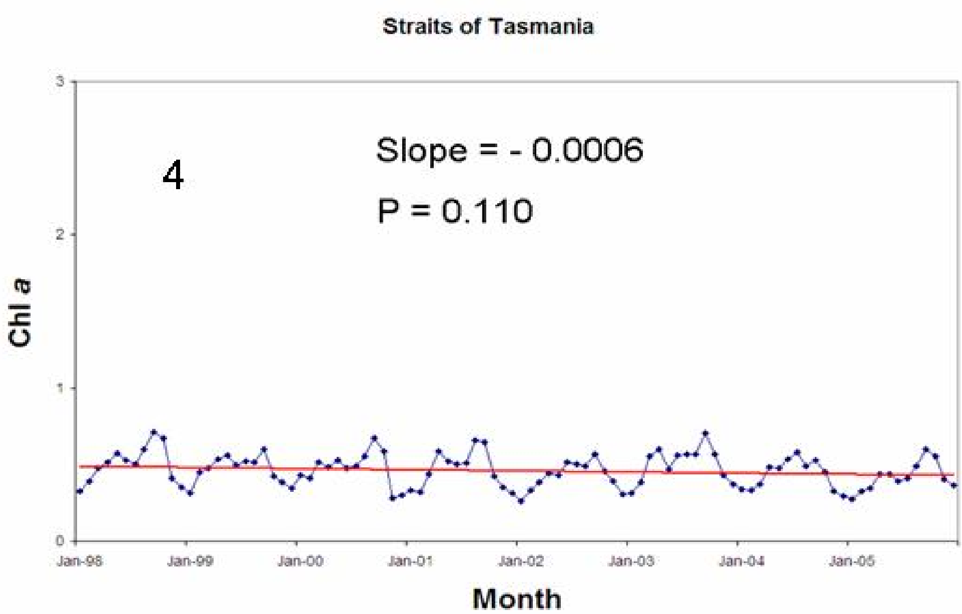
Straits of Tasmania
4
Slope = - 0.0006
P = 0.110
Chl a
3
2
1
0
Jan-98
Jan-99
Jan-00
Jan-01
Jan-02
Jan-03
Jan-04
Jan-05
Month

Figure 4

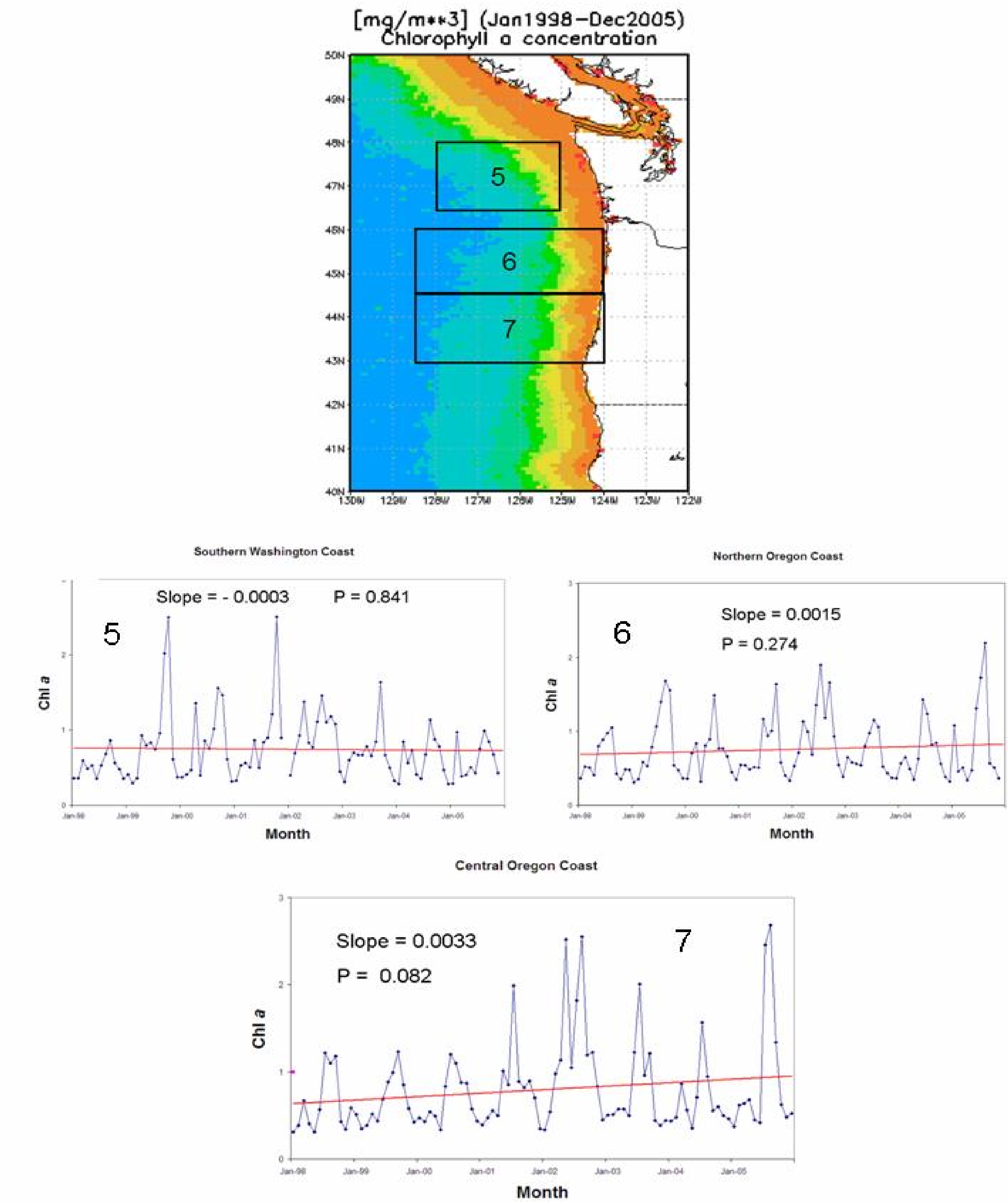
[mg/m**3] (Jan1998-Dec2005)
Chlorophyll a concentration
5
6
7
Southern Washington Coast
Slope = - 0.0003
P = 0.841
5
Chl a
Month
Northern Oregon Coast
Slope = 0.0015
P = 0.274
6
Chl a
Month
Central Oregon Coast
Slope = 0.0033
P = 0.082
7
Chl a
Month

Figure 5

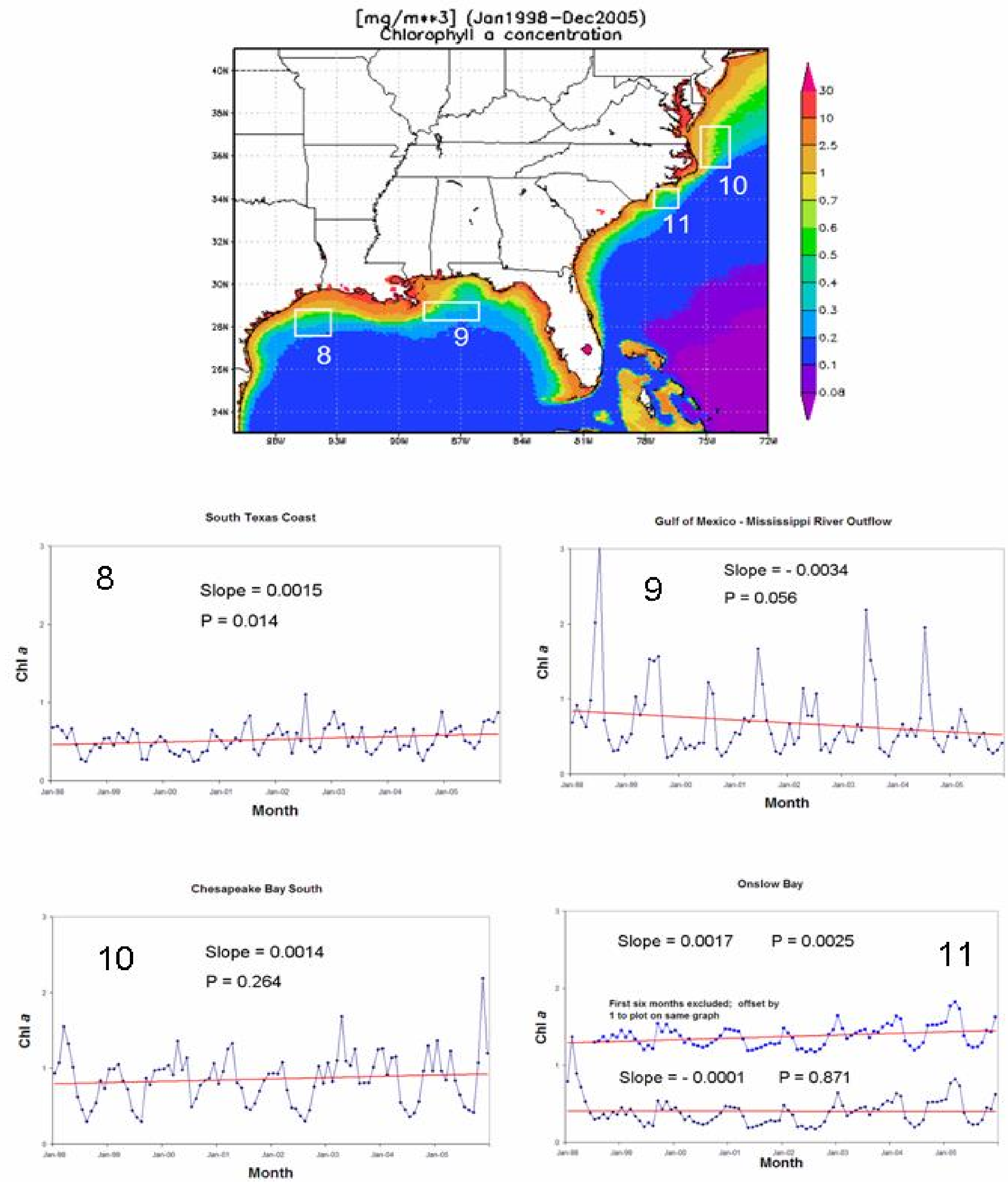

[mg/m**3] (Jan1998-Dec2005)
Chlorophyll a concentration
8
9
10
11
South Texas Coast
8
Slope = 0.0015
P = 0.014
Chl a
Month
Gulf of Mexico - Mississippi River Outflow
9
Slope = - 0.0034
P = 0.056
Chl a
Month
Chesapeake Bay South
10
Slope = 0.0014
P = 0.264
Chl a
Month
Onslow Bay
Slope = 0.0017
P = 0.0025
11
First six months excluded; offset by 1 to plot on same graph
Slope = - 0.0001
P = 0.871
Chl a
Month

Figure 6

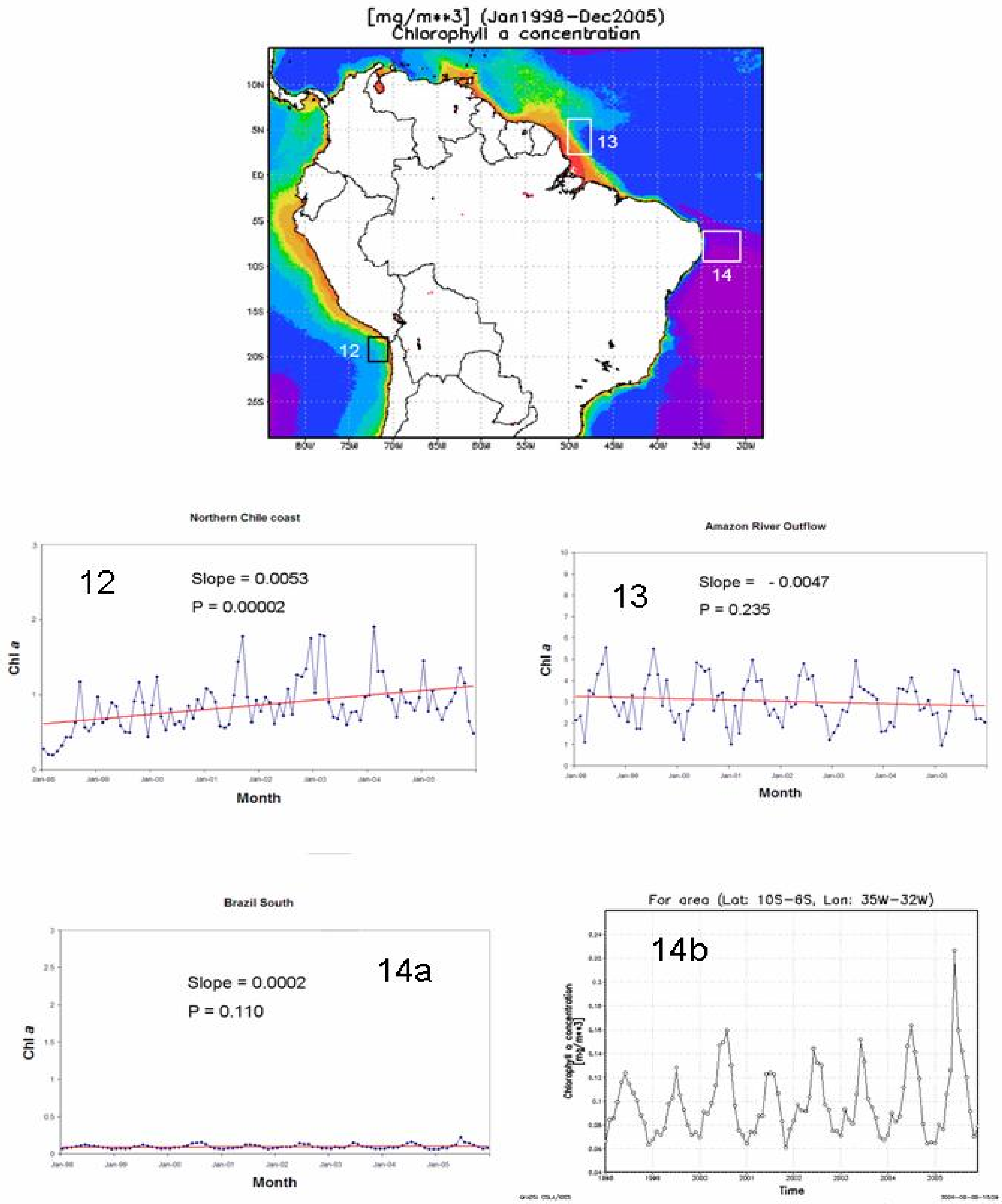
[mg/m**3] (Jan1998-Dec2005)
Chlorophyll a concentration
13
14
12
Northern Chile coast
12
Slope = 0.0053
P = 0.00002
Chl a
Month
Amazon River Outflow
13
Slope = - 0.0047
P = 0.235
Chl a
Month
Brazil South
Slope = 0.0002
P = 0.110
14a
Chl a
Month
For area (Lat: 10S-6S, Lon: 35W-32W)
14b
Time
Generated by NASA's Giovanni (giovanni.gsfc.nasa.gov)

Figure 7

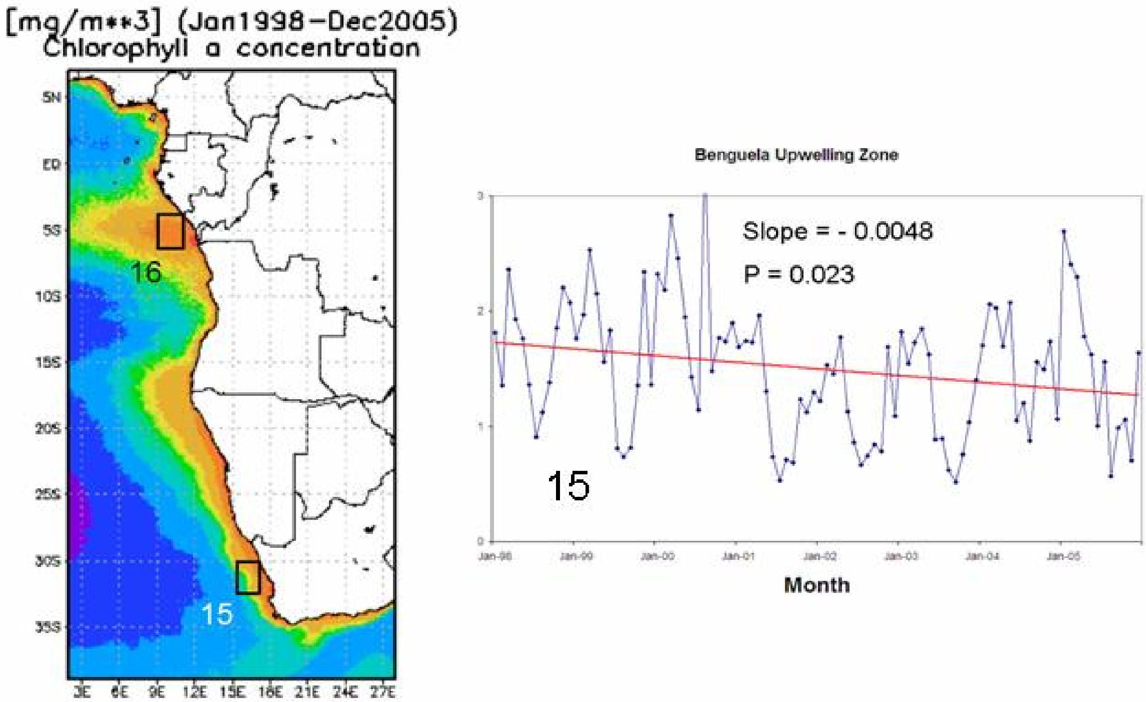

[mg/m**3] (Jan1998-Dec2005)
Chlorophyll a concentration
16
15
Benguela Upwelling Zone
Slope = - 0.0048
P = 0.023
15
Month

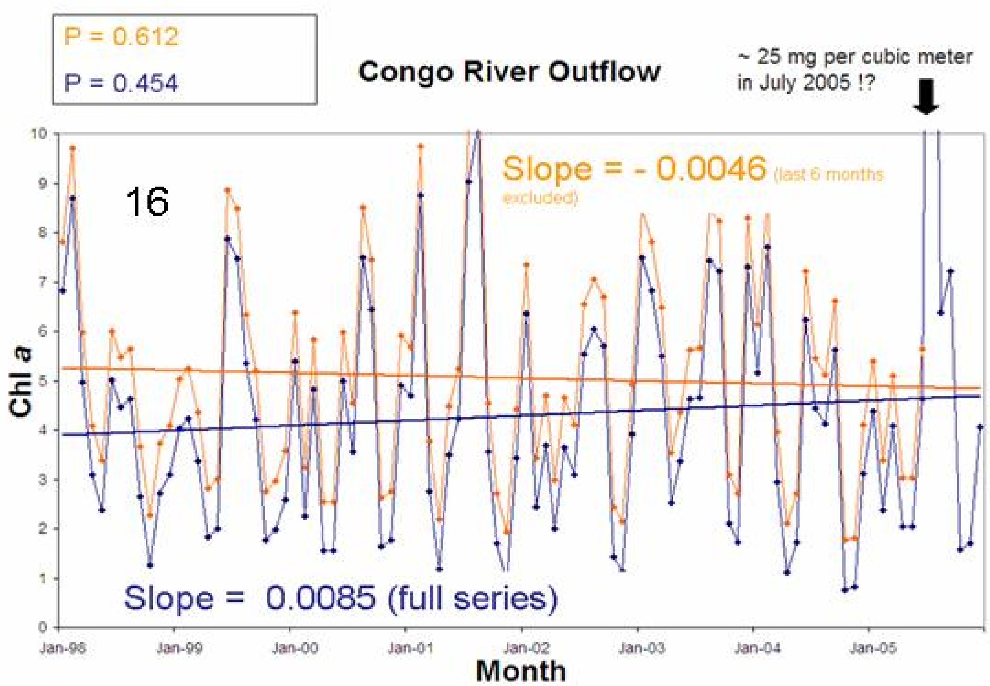

P = 0.612
P = 0.454
Congo River Outflow
~ 25 mg per cubic meter
in July 2005 !?
Slope = - 0.0046 (last 6 months excluded)
16
Chl a
Slope = 0.0085 (full series)
Month

Figure 8

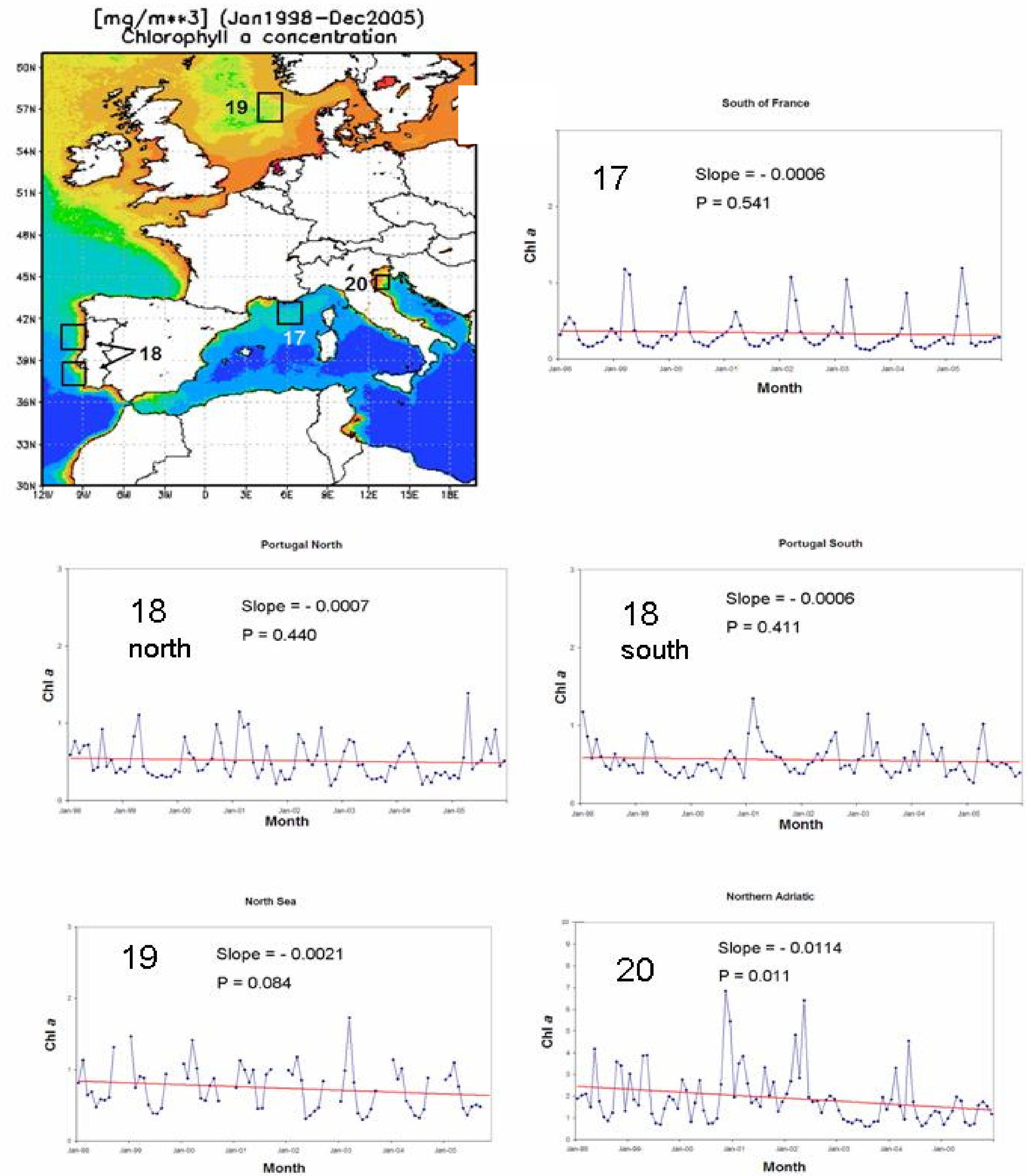

[mg/m**3] (Jan1998-Dec2005)
Chlorophyll a concentration
19
20
17
18
South of France
17
Slope = - 0.0006
P = 0.541
Chl a
Month
Portugal North
18
north
Slope = - 0.0007
P = 0.440
Chl a
Month
Portugal South
18
south
Slope = - 0.0006
P = 0.411
Chl a
Month
North Sea
19
Slope = - 0.0021
P = 0.084
Chl a
Month
Northern Adriatic
20
Slope = - 0.0114
P = 0.011
Chl a
Month